Available online at www.sciencedirect.com
SCIENCE DIRECT®
Journal of Power Sources 157 (2006) 584–591
JOURNAL OF POWER SOURCES
www.elsevier.com/locate/jpowsour

In situ STM studies of zinc in aqueous solutions containing PEG DiAcid inhibitor: Correlation with electrochemical performances of zinc–air fuel cells

Tzipi Cohen-Hyams [a,1], Yuli Ziengerman [b], Yair Ein-Eli [a,*]

[a] *Department of Materials Engineering, Technion-Israel Institute of Technology, Haifa 32000, Israel*
[b] *Electric Fuel Batteries Ltd., Arotech Corp., Bet Shemesh 99000, Israel*

Received 2 March 2005; accepted 22 July 2005
Available online 14 November 2005

Abstract

Electrochemical performance of prismatic zinc–air fuel cells comprising zinc anode gel containing poly(ethylene glycol) (PEG 600) and poly(ethylene glycol) bis(carboxymethyl) ether (PEG DiAcid 600) as corrosion inhibitor were studied. It was found that in addition to the low zinc corrosion rates obtained from cells utilizing PEG DiAcid 600 as corrosion inhibitor, both analog and global mobile system (GSM) discharge capacities and potential plateaus, in a wide range of temperatures were higher once PEG DiAcid was added to the zinc gel mixtures. The results obtained from in situ scanning tunneling microscopy (STM) studies of zinc substrates immersed in deionized (DI) water containing inhibitors reveal that the film produced on the zinc metal in the presence of PEG DiAcid is by far thinner than the film produced by other inhibitors such as PEG 600 and polyoxyethylene alkyl phosphate ester acid (GAFAC RA 600). These studies also reveal that the addition of PEG DiAcid forms an adherent and a complete protective coverage, while the addition of PEG 600 and GAFAC RA 600 resulted in an incomplete coverage with the appearance of pits and terraces, indicating on a restricted inhibition performance of these two polymers compared with PEG DiAcid. These studies suggest a low interface resistivity of zinc immersed in alkaline solution containing PEG DiAcid, which is expressed in a higher working potential and increased cell capacity in different temperatures at two discharge modes of analog and GSM.

Keywords: PEG DiAcid; Zinc; Corrosion; Inhibitors; Zinc–air cells; Analog and GSM

1. Introduction

Alkaline batteries and zinc–air cells based on zinc anode are still highly attractive since they are capable of providing relatively high discharge capacity with high efficiency. Zinc anode gels in alkaline cells are prone to electrochemical corrosion reactions when stored at or above room temperature. The corrosion rate increases as the storage time and temperature rises and can lead to a dramatic decrease in cell capacity. Alkaline electrolyte in the anode gel corrodes the zinc anode upon contact, forming oxidized zinc products that decrease the availability of active zinc while simultaneously generating hydrogen gas.

Hydrogen gas generated in such reactions can increase the internal cell pressure causing electrolyte leakage and disrupt cell integrity. Hydrogen gas generated at the anode zinc surface is accelerated when the battery is partially discharged, thereby leading to a pressure built-up and eventually to electrolyte leakage. The corrosion reactions leading to hydrogen evolution involve electrochemical active sites on the zinc anode surface. Such sites can include surface and bulk metal impurities, surface lattice features, grain boundary features, lattice defects, point defects and inclusions. In order to minimize undesirable corrosion and gassing during storage, efforts are made in order to reduce the presence of impurities in the anode and the electrolyte as well as employing corrosion-resistant zinc alloys. Zinc metal is alloyed with three to four elements at low concentrations (20–1000 ppm) during the thermal production process of the powder. This zinc alloyed powder is used as the anode of choice in alkaline (Zn/MnO_2) and zinc–air cells. The elements added to the zinc metal are commonly Al (20–150 ppm),

* Corresponding author. Tel.: +972 4 829 4588; fax: +972 4 829 5677.
E-mail address: eineli@tx.technion.ac.il (Y. Ein-Eli).
[1] Present address: Department of Materials Science and Engineering, University of California, Berkeley, CA 94720, USA.

0378-7753/$ – see front matter © 2005 Elsevier B.V. All rights reserved.
doi:10.1016/j.jpowsour.2005.07.090

Bi (50–200 ppm), Ca (100–500 ppm) and In (200–1000 ppm) [1–4]. While all the elements are added in order to improve the electrochemical behavior of the discharged cell (for example, shorts prevention, decrease in the ohmic cell resistance and decrease in the self-discharge rate while the cell is being partially discharged), and to suppress the anodic reaction of zinc, still there is a need to add another component to the electrolyte which is capable of reducing the zinc corrosion in the alkaline media. Overcoming the corrosion of the zinc anode in the alkaline media without the use of mercury, which is considered to be a highly efficient zinc corrosion inhibitor, is a crucial issue. Thus, the development and studying of organic polymeric inhibitors capable of replacing mercury and mercury salts without any degradation of the zinc anode performance or the overall alkaline cell electrochemical characteristics is highly important [5–24].

Organic surfactants and inorganic corrosion-inhibiting agents are commonly added to the zinc anode gels. The role of these organic additives is to form hydrophobic film that protects the zinc anode surface during storage, forming efficient anode–electrolyte interface. The efficiency of these polymeric compounds to enhance the corrosion resistance of zinc depends on their chemical structure, concentration and their stability in the electrolyte. Many of the inhibitors studied so far share a common feature: they all posses the same backbone tail composed of polyoxyethylene moiety ($-O-CH_2-CH_2$). Each of the inhibitor has a different terminating "head". For example, poly(ethylene glycol) is terminated at both ends with –OH group, while polyoxyethylene alkyl phosphate ester acid is terminated with −POOH group.

In previous communications [23,24], we reported on the superiority a substitute di-carboxylic acid PEG (we term this polymeric compound in abbreviation as "PEG DiAcid" throughout the paper) and the inferior results obtained by adding this material into the alkaline electrolyte. The carboxylic terminating groups exist in the alkaline media as carboxylate anions, and hence a possibility of enhanced binding in the form of two binding sites or "fingers" to the zinc metal would take place.

This paper reports on the application of PEG DiAcid zinc inhibitor in commercial prismatic zinc–air cells. Corrosion rates of these cells, electrochemical performance (discharged at different current characteristics [analog and global system for mobiles (GSM)] along with STM observation on the adsorbtion nature of PEG DiAcid compared with PEG and GAFAC RA600 and its correlation with the electrochemical performances are reported.

2. Experimental

2.1. In situ scanning tunneling microscopy (STM) studies

Electrolytes were prepared by dissolving 2000 ppm of different polymers, poly(ethylene glycol) [PEG 600; Aldrich], poly(ethylene glycol) bis(carboxymethyl) ether [PEG DiAcid 600; Aldrich] and polyoxyethylene alkyl phosphate ester acid form [GAFAC RA 600; Aventis-Sanofi (Rhône-Poulenc)] in deionized (DI) water (with a measured conductivity of less than 2 $\mu S\,cm^{-1}$). All electrolytes were prepared via the addition of the desired amount of the organic inhibitor from a dilute solution containing 5% of the tested organic polymer in water. Pure metal zinc (Zn, 99.997%, Umicore) samples were mirror polished with the final use of 0.05 μm alumina suspension prior to immersion in the tested solutions. STM experiments were conducted using a PicoSPM from Molecular Imaging. Tunneling tips were made of a platinum–iridium (9:1) wire (250 μm thick) coated with a wax (produced by Molecular Imaging). The tunneling scanning current was set to 0.3 nA.

2.2. Zinc–air cell components and assembly

Zinc anode gel was prepared by mixing 60% (w/o) Zn powder (ABI, Mitsui), 0.5% (w/o) acrylic acid polymer [$-(CH_2-HCCOOH)_n$] as a gelling agent [(carbopol 941), Goodrich] with a molecular weight of −1,250,000), 800 ppm PEG 600 or PEG DiAcid 600 in 8.0 M KOH solution containing 22 $g\,l^{-1}$ zincate (ZnO, Aldrich). Air cathode was produced from a mixture of active carbon powder with a manganese oxide catalyst powder and PTFE binder, compressed onto a woven nickel mesh, and laminated to a porous Teflon film blocking layer. Zinc air cells contained 8 g of the prepared gel, corresponding to a theoretical capacity of 4.0 Ah. Prismatic zinc–air cells with a total weight of 12.8 g were produced by Electric Fuel Ltd. (scheme and dimensions are illustrated in Scheme 1).

2.3. Zinc–air cell corrosion rate analysis

Corrosion rates were calculated based on gas chromatograph (GC, Gow-Mac, series 580) measurements conducted at 50 °C at certain depth of discharge (DOD) stages of 0, 20, 50 and 85% (0, 0.8, 2 and 3.4 Ah, respectively). Captured gas from the glass container encapsulating zinc–air cells was injected into the GC chamber during 8–10 h of measurements. Corrosion rate (percent of weight Zn loss per week) was calculated from plotting a graph of produced hydrogen volume (ml) versus measurement time (min).

2.4. Zinc–air cells discharge

Cells were subjected to two different discharge modes: analog (galvanostatically at 0.47 A) and GSM (continues pulsing of 2 A for 0.5 ms and 0.2 A for 3.5 ms, yielding an average current of 0.425 A). Although the average current density in GSM discharge mode is lower than analog current discharge, the short duration high current pulses of 2 A introduces extreme operational conditions for the electrochemical cell. Electrochemical studies were carried out with MACCOR 2000 battery cycler 30 days subsequent to cell production. During this storage time all cells were taped stored at room temperature (22 ± 2 °C). Electrochemical performance of zinc–air cells were performed in a controlled environmental chamber (Thermotron 2800) at 50% relative humidity (RH). Each set of measurements was carried out with five cells from each group.

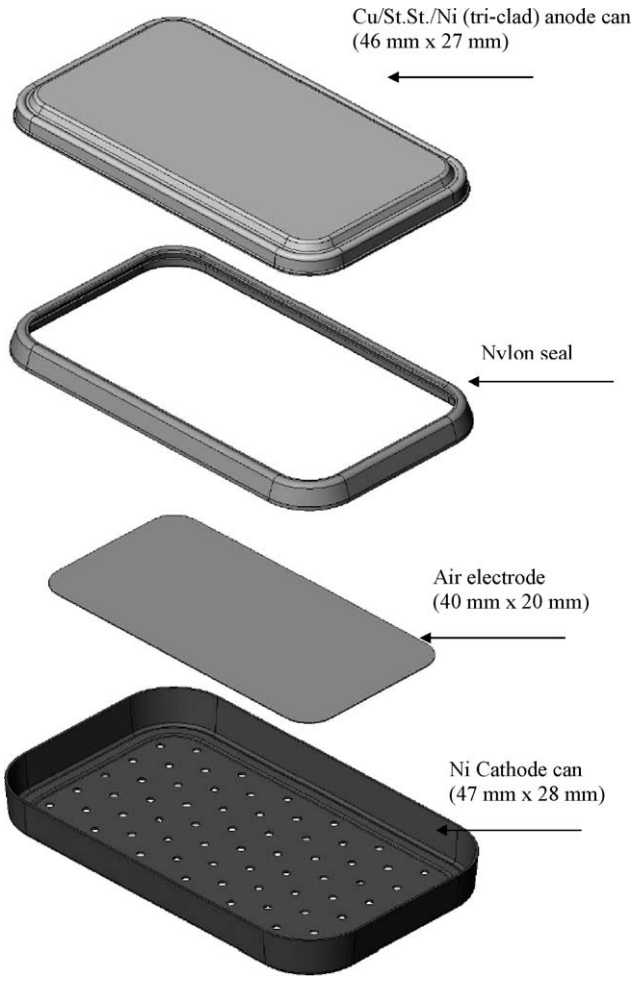

Scheme 1. Prismatic zinc–air cell components and construction.

3. Results and discussion

3.1. Surface studies of Zn in DI water containing inhibitors

Fig. 1 presents STM image of zinc surface in air, scanned immediately subsequent to polishing, indicating the rapid formation of oxides at the zinc surface. Fig. 2a–c presents in situ STM images (0.5 μm × 0.5 μm) of zinc immersed in DI water containing PEG 600, PEG DiAcid and GAFAC RA 600, respectively. Zinc surface is covered with an organic film immediately upon immersion. The morphology developed at the zinc surface in the presence of all the inhibitors is consistent with time, and does not change even after 8 h. The major distinction detected is the growing thickness of the produced film on the zinc with time in solutions containing PEG 600 and GAFAC RA 600, while the film produced at the zinc surface in the presence of PEG DiAcid's remained smooth and very thin. Adsorption morphologies formed by the inhibitors were stable within 1 h of immersion without significant changes. Thus, the results in this report will refer to the film adsorption morphology after 1 h. It is also noted that in general, the inhibition film tends to smooth the surface, introducing difficulties in identifying grain boundaries.

The STM results shown in Fig. 2 are with an excellent agreement with the electrochemical results reported previously

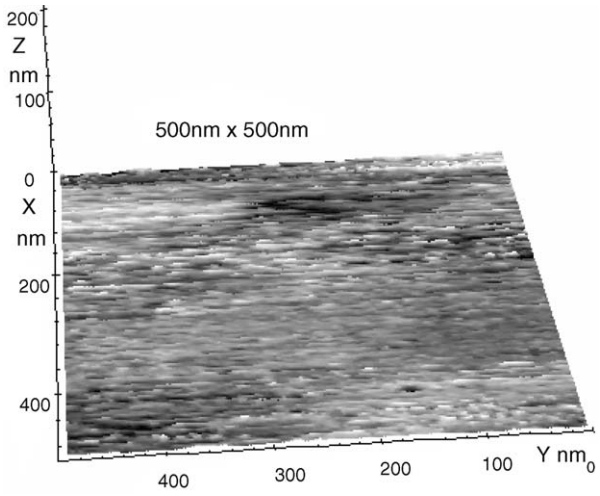

Fig. 1. A 3D STM image of a zinc surface in air, scanned immediately subsequent to polishing at 0.5 μm × 0.5 μm.

[20–24]. Among the three inhibitors studied, PEG DiAcid presented an excellent absorbance, while GAFAC RA 600 showed the poorest surface coverage. PEG DiAcid presented a perfect coverage, very thin, dense film, with a complete surface coverage (Fig. 2b). However, the use of PEG 600 and GAFAC RA 600 in the aqueous solution resulted in imperfect coverage, with exposed bare zinc sites and even terraces, indicating a restricted inhibition performance of these two polymers compared with PEG DiAcid, as was demonstrated in previously reported polarization behavior [21,24]. The addition of 2000 ppm PEG 600 resulted immediately in almost full coverage, though the film was not smooth with small terrace features and holes (Fig. 2a). The addition of GAFAC RA 600 resulted in a relatively rough surface with high terraces that showed large areas of uncovered bare zinc (Fig. 2c). Thus, the inhibitor seems to be effective only at a portion of the zinc surface.

STM images of the surface roughening that occurs during oxidation of zinc in air (Fig. 1) indicate that the zinc surface root mean square (rms) of the zinc surface almost did not change with the addition of 2000 ppm PEG DiAcid, while the surface roughness increased considerably with the addition of 2000 ppm PEG 600 and GAFAC RA 600. This increase is by at least one order of magnitude than for zinc surface rms in pure water was measured. The rms of the zinc surface in pure water was measured to be 40.5 ± 17.3 Å, and it changed to 78.6 ± 25.1, 245 ± 81.9 and 522.2 ± 172 Å with the addition of 2000 ppm, PEG DiAcid, PEG 600 and GAFAC RA 600, respectively (for a scan rate of 0.5 μm × 0.5 μm). In addition, in situ observations (Fig. 2) showed not only a full and dense coverage of the film developed in the presence of PEG DiAcid, but also a similar morphology to the zinc metal surface, meaning that PEG DiAcid adsorbed as a few mono-layers only. It seems that the addition of PEG DiAcid forms an adherent and a complete protective coverage.

3.2. Zn morphology in the presence of PEG DiAcid

Previous morphological (AFM) and spectroscopic studies of zinc metal in a strong alkaline solution (8.5 M KOH) in the

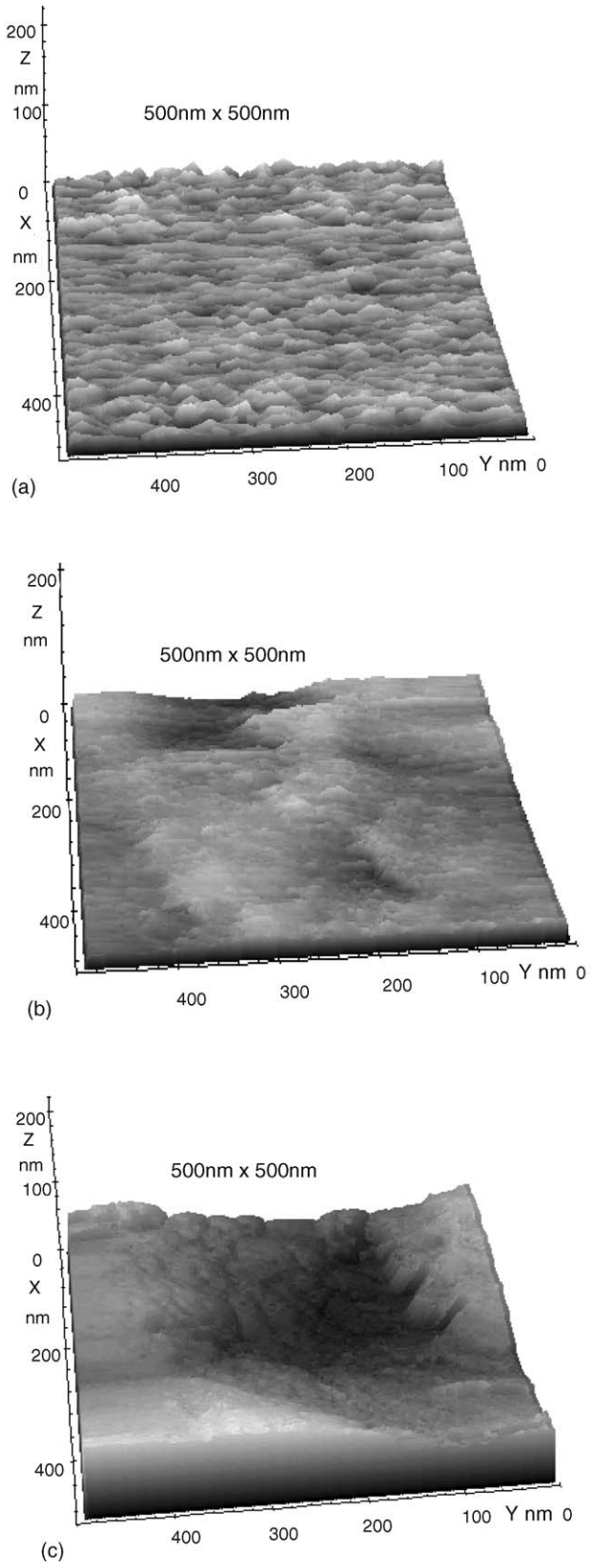

Fig. 2. In situ 3D STM images of zinc surfaces in DI water containing 2000 ppm of: (a) PEG DiAcid; (b) PEG 600; (c) GAFAC RA 600.

presence of PEG DiAcid [24] indicated that at concentrations of 2000 ppm, a full and homogeneous coverage of the zinc surface is obtained, supporting our STM results. The film developed on the zinc metal in the presence of 2000 ppm of PEG DiAcid 600 in alkaline solution was characterized as a relatively thick; the surface morphology formed was not smooth but could be considered as uniformed. In addition, based on FTIR data, obtained from zinc immersion in a neat solution of PEG DiAcid it was concluded that the interaction between the organic polymer and the zinc is performed only via one carboxylic head, while the second carboxylate head is positioned at the zinc/alkaline interface, facing the solution [22]. The reason for the discrepancy in the morphological characteristics lies in the different electrolyte used in the present study. While the previous studies [23,24] utilized a strong alkaline (8.5 M KOH) solution, in this report we present inhibition performance in only deionized water, without additional ions (such as hydroxides and zincates). Thus, the morphology detected in aqueous solution containing only inhibitor cannot be attributed to heavy formations and deposition of zinc hydroxide, oxide and zincates at the zinc interface, as expected in a an alkaline media. It is expected that PEG DiAcid is present in both solutions (DI and alkaline) as di-anion, contributing to increased solution conductivity, thus allowing higher mobility of PEG DiAcid to the Zn surface. It is reasonable to expect, based on the STM results presented in Fig. 2 that the thin and compact film produced at the zinc surface is most probably due to a double carboxylate binding of a single PEG DiAcid molecule.

3.3. Zn morphology in the presence of PEG 600

The morphological characteristics of PEG 600 resemble previous studies, though the film produced in pure DI water are less uniform and consisted of much larger uncovered zinc areas. A proposed structure of the adsorbed film recall for an ordered self-assembled structure or a branch hydrocarbon with bulky hydrocarbon groups that form a “brush” type structure, as described elsewhere [22]. The reason for a partial coverage of PEG 600 in DI water versus alkaline, in addition to the fact that the presence of hydroxide and zincate ions is eliminated, is the lower conductivity of the polymer itself.

PEG 600 has two functional groups, and in a strong alkaline solution (8.5 M KOH) a higher solvation of the polymer occurs, leading to a better coverage of the zinc surface. The role of PEG 600 depends also on its mobility in the electrolyte: in water, hydrogen bonds are formed between the water and the oxygen atoms of one PEG 600 molecule [25]. Adsorption of PEG or PEG^{-} anion competes with oxide (or hydroxide) adsorption. In a concentrate alkaline solution, when the amount of water is substantially reduced, the water molecules bind with two PEG molecules, thereby reducing the mobility of both water and the PEG polymer [26]. Diffusion of the complexes (Zn^{2+}, ROH) in the solution is promoted when the water content in the solution is high. Thus, in solutions with higher concentration of KOH, PEG is less mobile and adsorption kinetic on the surface will be slow while zinc hydroxide and zincate formation will be promoted due to the presence of high alkaline and dissolved ZnO concentration.

3.4. Zn morphology in the presence of GAFAC RA 600

Previous spectroscopic studies in a strong alkaline media [22] showed that the active polymer in GAFAC RA 600 mixture is actually the monoester and not the di-ester, and that the active site is the phosphonium polymer head. The defected zinc morphology in the form of steps and terraces having bare zinc sites in the presence of GAFAC RA 600 observed in this study is probably due to a partial ionization of the phosphonium anion in pure water. Since the conductivity is low, and GAFAC RA 600 has wider stereo-groups, the polymer adsorbs partially to the zinc surface, thus showing poorer inhibition performance. Another reason may be a steric interruption by the molecular structure of GAFAC RA 600. Once a steric problem is introduced in the shape of the larger POO^- end group, the probability of water interacting with the zinc surface is enhanced, leading to an increase in the film roughness. The non-uniformity coverage of the inhibitor over the surface may be due to the preferential adsorption of the inhibitor on certain ($h\,k\,l$) facets. The terrace features may indicate that the adsorption of GAFAC RA 600 occurs heterogeneously at the surface, probably favoring certain low index $h\,k\,l$ planes.

4. Electrochemical performance of zinc–air cells utilizing PEG DiAcid and PEG 600

4.1. Analog discharge as a function of temperature

Fig. 3a–d presents analog discharge profiles obtained from zinc–air cells at different temperatures (22, 10, 5 and 0 °C, respectively) utilizing PEG DiAcid and PEG 600 as the inhibitor of choice in the gel composition. As can be seen, the use of PEG DiAcid provides superior electrochemical cell behavior; in all temperatures the working potential, and thus the measured capacity obtained from discharging zinc–air cells employing PEG DiAcid are significantly higher once compared with the data obtained from zinc–air cells utilizing PEG 600 (observe also Table 1, summarizing this experimental work). A gap of 30 mV between cell's working potentials is observed which is translated into a capacity gap of 0.3–0.4 Ah between the two cells type. In addition, Table 1 indicates that for both cells the lower possible working temperature is around 0 °C. Lowering the temperature to −5 °C causes a major reduction in cells performance, most probably due to a reduced electrolyte conductivity and increased interfacial resistance. However, even at the temperature of −5 °C, both capacity and working potential obtained

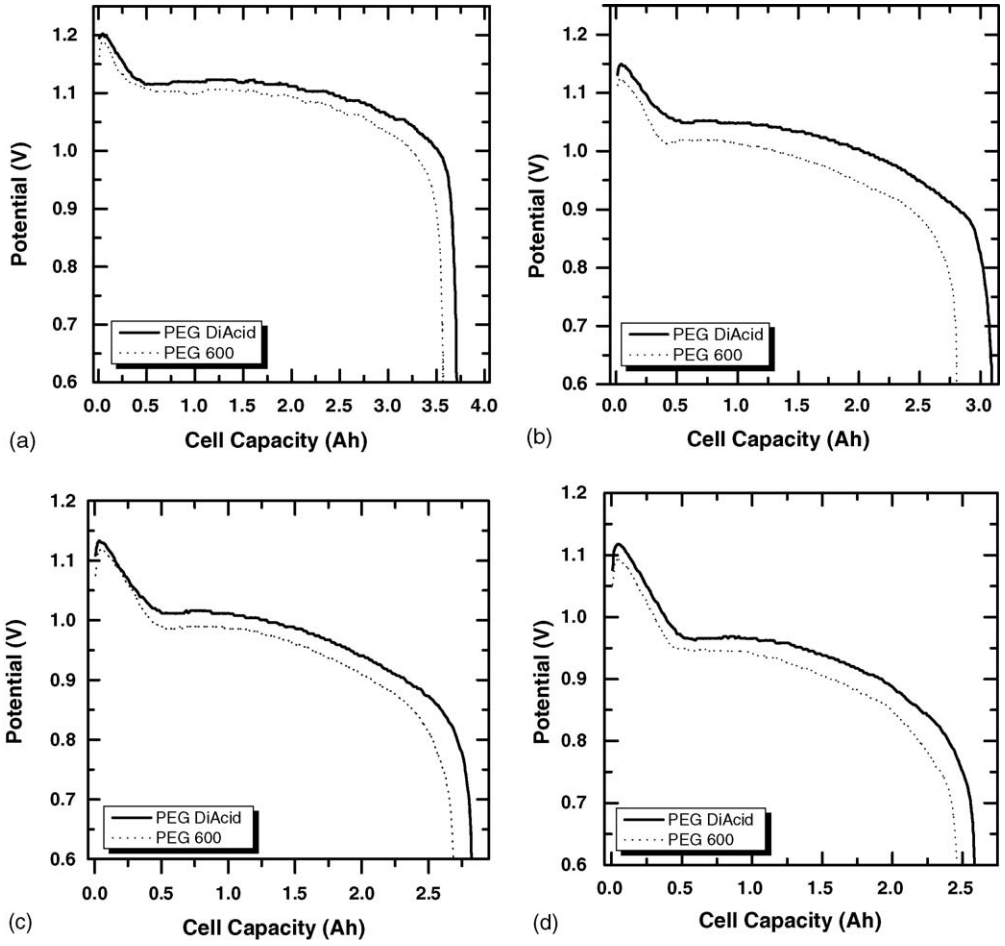

Fig. 3. Potential (V)–capacity (Ah) profiles obtained from analog discharge mode (0.47 A) of zinc–air cells utilizing PEG 600 and PEG DiAcid as their corrosion inhibitors at: (a) room temperature (22 °C); (b) 10 °C; (c) 5 °C; (d) 0 °C.

Table 1
Performance of zinc–air cells containing PEG 600 or PEG DiAcid 600 corrosion inhibitors as a function of temperature in analog (0.47 A) operation mode

T (°C)	PEG 600		PEG DiAcid 600	
	Capacity (Ah)[a]	Potential plateau (V)	Capacity (Ah)[a]	Potential plateau (V)
22	3.5 ± 0.15	1.09 ± 0.02	3.7 ± 0.2	1.13 ± 0.02
10	2.75 ± 0.2	1.01 ± 0.02	2.95 ± 0.2	1.05 ± 0.02
5	2.45 ± 0.1	0.97 ± 0.03	2.75 ± 0.15	1.01 ± 0.02
0	2.1 ± 0.15	0.93 ± 0.02	2.45 ± 0.2	0.97 ± 0.02
−5	0.65 ± 0.1	0.88 ± 0.01	0.95 ± 0.1	0.91 ± 0.02

[a] Capacity was measured to a cut-off potential of 0.8 V.

from cells utilizing PEG DiAcid are higher than the corresponding values measured from cells utilizing PEG 600.

4.2. GSM discharge as a function of temperature

Fig. 4a–d presents GSM discharge profiles obtained from zinc–air cells at different temperatures (22, 10, 5 and 0 °C, respectively) utilizing PEG DiAcid and PEG 600 as the inhibitor of choice in the gel formulation. As can be seen, again, the use of PEG DiAcid provides superior electrochemical cell behavior; in all temperatures the working potentials are higher, both at low and high pulses, and thus the measured capacity obtained from discharging zinc–air cells employing PEG DiAcid are significantly higher once compared with the GSM data obtained from zinc–air cells utilizing PEG 600 (observe also Table 2, summarizing our measurements). The strong impact of PEG DiAcid is shown once the cells are being discharged in high pulse mode. At this mode, a discharge current of 2 A flows in the cells and as can be seen, not only the working potential plateau is higher but also the potential dip observed within 10–15% of discharge time is much shallower.

4.3. Discharge behavior of zinc–air cells subsequent to 30 days storage at 71 °C

In order to further study the impact of the inhibitor on zinc–air cell performance we stored two groups of zinc–air cells utilizing both organic inhibitor at 71 °C. The cells were glue taped during the storage period and were discharged at the end of the 30 days period at room temperature (22 °C) in two discharge modes, analog (Fig. 5a) and GSM (Fig. 5b). It is expected that both storage and aging at elevated temperature would accelerate undesired processes, especially acceleration of cell corrosion rate, thus leading to a decreased capacity and low working potential due to internal pressure built-up in the cells. Surprisingly, zinc–air cells utilizing PEG DiAcid as a corrosion inhibitor do not suffer

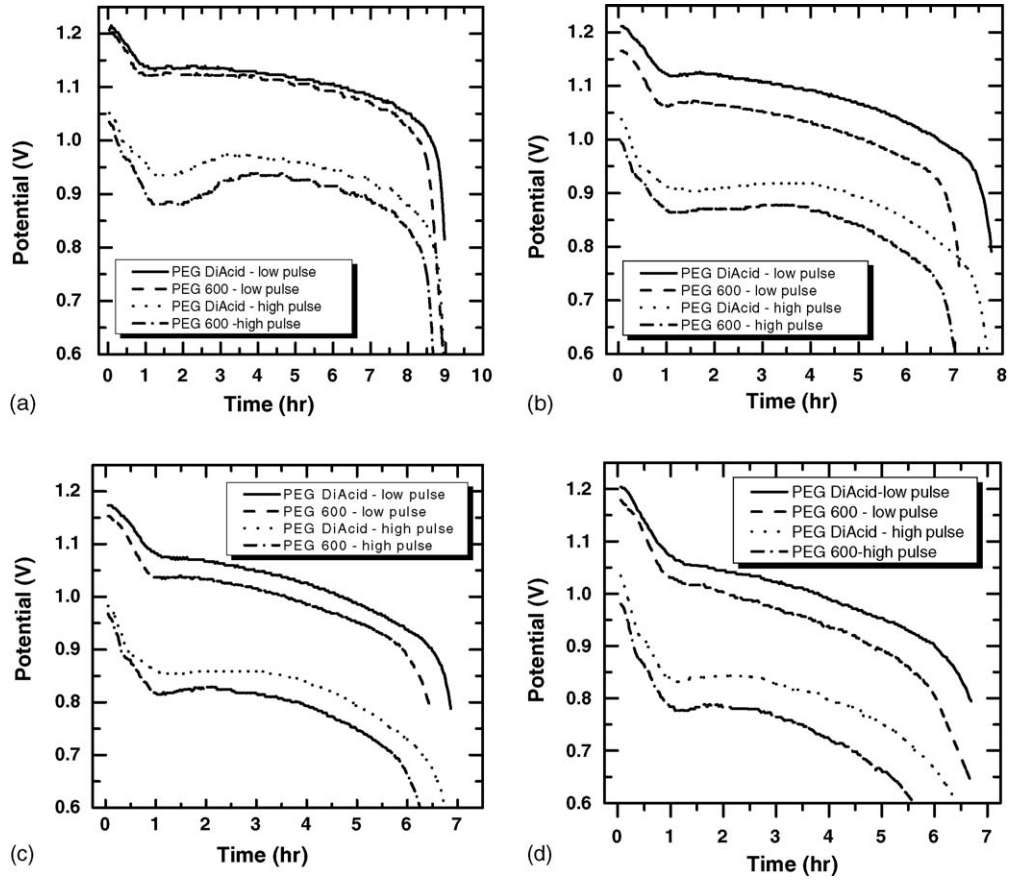

Fig. 4. Potential (V)–time (h) profiles obtained from global system mobile (GSM) discharge mode (low pulse—0.2 A for 3.5 ms; high pulse—2 A for 0.5 ms) of zinc–air cells utilizing PEG 600 and PEG DiAcid as their corrosion inhibitors at: (a) room temperature (22 °C); (b) 10 °C; 5 °C; (d) 0 °C.

Table 2
Performance of zinc–air cells containing PEG 600 or PEG DiAcid 600 corrosion inhibitors as a function of temperature in GSM (2/0.2 A) operation mode

T (°C)	PEG 600			PEG DiAcid		
	Capacity (Ah)[a]	Potential plateau (V)	Potential dip (V)	Capacity (Ah)[a]	Potential plateau (V)	Potential dip (V)
22	3.6 ± 0.2	0.91 ± 0.02	0.87 ± 0.02	3.8 ± 0.15	0.96 ± 0.02	0.94 ± 0.02
10	3.0 ± 0.15	0.87 ± 0.02	0.84 ± 0.02	3.3 ± 0.2	0.92 ± 0.02	0.91 ± 0.02
5	1.7 ± 0.2	0.82 ± 0.01	0.81 ± 0.01	2.15 ± 0.1	0.86 ± 0.01	0.85 ± 0.01
0	0.42 ± 0.1	0.78 ± 0.01	0.77 ± 0.01	1.7 ± 0.1	0.85 ± 0.02	0.83 ± 0.02
−5	0.15 ± 0.1	0.72 ± 0.02	0.71 ± 0.02	0.45 ± 0.1	0.75 ± 0.01	0.73 ± 0.01

[a] Capacity was measured to a cut-off potential of 0.8 V.

from a prolong storage at elevated temperature. It is shown that both capacity and working potential in analog and GSM discharge modes not only that were not badly effected but rather were improved upon aging at elevated temperature (compare with the behavior shown in Fig. 3), while zinc–air cells utilizing PEG 600 as the corrosion inhibitor suffer from a lower working potentials (analog and GSM) and reduced capacity under extreme discharge mode of GSM.

The use of PEG DiAcid with its capability to form a thin compact protective layer as was shown in our earlier STM studies may be the reason for the enhanced electrochemical performance of zinc–air cells utilizing this superior inhibitor, even in extreme conditions (low temperature, elevated temperature aging and high discharge current pulses).

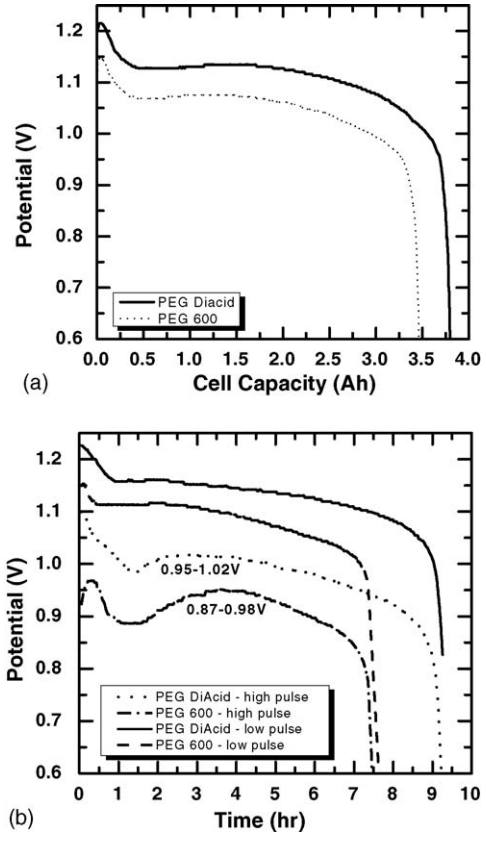

Fig. 5. Zinc–air cells performances utilizing PEG 600 and PEG DiAcid as their corrosion inhibitors subsequent to 30 days storage at 71 °C: (a) potential (V)–capacity (Ah) profiles obtained from analog discharge mode (0.47 A) and (b) potential (V)–time (h) profiles obtained from global system mobile (GSM) discharge mode (low pulse—0.2 A for 3.5 ms; high pulse—2 A for 0.5 ms).

4.4. Corrosion rates at accelerated temperatures

In our previous studies, we presented electrochemical polarization studies indicating the superiority of PEG DiAcid as the inhibitor of choice in electrochemical cells utilizing non-alloyed zinc working electrode. In this study, we evaluate the corrosion rate of alloyed zinc (ABI) gel in zinc–air cells utilizing both PEG 600 and PEG DiAcid at different analog DOD stages (0, 0.8, 2 and 3.4 Ah) by an indirect evaluation of hydrogen evolution from the zinc–air cell as a function of time, as outlined in Section 2. Partial discharged alkaline cells and zinc–air batteries suffer from increased corrosion rates, most probably due to the formation of zincates at the zinc interface, as a cell discharge product. Fig. 6 presents corrosion rates measured at 50 °C of partially discharged cells utilizing both PEG 600 and PEG DiAcid in their zinc gel formulation. As can be seen, at a fully charged state, corrosion rates measured from both type of cells are identical and quite depleted. In a partial discharge cell with a DOD of 20% (0.8 Ah discharge capacity) a small but significant gap is observed between the corrosion values measured from both type of cells. This gap is further increased in a 50% DOD of 2 Ah, while eventually an almost complete discharged cell (85% DOD, 3.4 Ah) utilizing

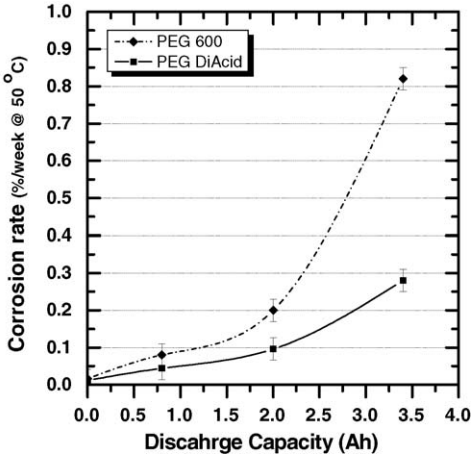

Fig. 6. Corrosion rate of zinc–air cells utilizing PEG 600 and PEG DiAcid as their corrosion inhibitors at 50 °C. Rate was measured by hydrogen evolution detected by gas chromatography (GC).

PEG DiAcid has reduced corrosion values (0.26% per week) in comparison to cells utilizing PEG 600 (0.82% per week). These measurements illustrate the wide versatility of PEG DiAcid as inhibitor; not only does it produce a thin and a compact protective layer on top of the zinc substrate, which in turn contributes to enhanced working potentials and capacities, but it also reduces cell corrosion once it is partially discharged.

5. Conclusion

PEG DiAcid forms an adherent film at the zinc interface, which provides a complete and protective coverage, while the presence of PEG 600 and GAFAC RA 600 resulted in an incomplete coverage with bare zinc sites, pits and terraces at the zinc surface. This leads to better performances of PEG DiAcid as zinc inhibitors compare with other inhibitors, as was demonstrated by comparisons of zinc–air cell performances. Not only that PEG DiAcid reduces cell corrosion, but also at the same time it causes an increase in the cell capacity and the working potential in a wide range of temperatures. In extreme GSM discharge mode (high current pulse of 2 A), the introduction of PEG DiAcid reduces the potential dip and extends the discharge time (capacity). The use of PEG DiAcid with its capability to form a thin compact protective layer, as was shown in STM images, is the reason for the enhanced electrochemical performance of zinc–air cells utilizing this superior inhibitor, even at extreme conditions of low temperature, elevated temperature aging and high discharge GSM current pulses.

Our study demonstrates the superiority and wide versatility of PEG DiAcid as inhibitor; it produces a thin, compact protective layer at the zinc substrate surface, which in turn contribute to enhanced working potentials and capacities. In addition, it also substantially reduces cell corrosion rates once it is partially discharged.

Acknowledgments

This research work was funded by Electric-Fuel Batteries, the Research Foundation of the Technion-Israel Institute of Technology and by the Miami Energy Fund, under Contract No. 2003446 framework. The authors would like to acknowledge the assistance of Mr. Iftach Hyams and Yaron Shrim in manuscript preparations.

References

[1] J.-Y. Huot, E. Boubour, J. Power Sources 65 (1997) 81.
[2] Y. Sato, M. Takahashi, H. Asakura, T. Yoshida, K. Tada, K. Kobayakawa, J. Power Sources 38 (1992) 317.
[3] M. Yano, S. Fujitani, K. Nishio, Y. Akai, M. Kurimura, J. Appl. Electrochem. 28 (1998) 1221.
[4] A.R.S. Kannan, S. Muralidharan, K.B. Sarangapani, V. Balaramachandram, V. Kapali, J. Power Sources 57 (1995) 93.
[5] J. Baur, A. Winkler, U.S. Patent 3,963,520 (1976).
[6] E.J. Rossler, F.J. Przybyla, U.S. Patent 4,195,120 (1980).
[7] P. Chalilpoyil, F.E. Parsen, C.C. Wang, U.S. Patent 4,777,100 (1988).
[8] C. Juhel, B. Beden, C. Lamy, J.M. Leger, R. Vignaud, Electrochim. Acta 35 (1990) 479.
[9] H. Yoshizawa, M. Akira, N. Yoshiaki, S. Sachiko, U.S. Patent 5,168,018 (1992).
[10] P. Chalilpoyil, H.S. Padula, P.B. Harris, R.B. Wo, G. Brual, F. Kasianowicz, U.S. Patent 5,401,590 (1995).
[11] M.S. Zubov, G.E. Kazakevitch, I.G. Basova, E.B. Kulikova, Russ. J. Appl. Chem. 67 (3–2) (1994) 425.
[12] V.K. Nartey, L. Binder, K. Kordesch, J. Power Sources 52 (1994) 217.
[13] C.B. Huang, Y.P. Xiong, L.X. Cao, X.J. Cao, J. Power Sources 63 (1996) 137.
[14] S. Manov, F. Noli, A.M. Lamazoure, L. Aries, J. Appl. Electrochem. 29 (1999) 995.
[15] D. Dobryszycky, S. Biallozor, Corros. Sci. 43 (2001) 1309.
[16] L.M. Baugh, F.L. Tye, N.C. White, J. Power Sources 9 (1983) 303.
[17] B. Szczesniak, M. Cyrankowska, A. Nowacki, J. Power Sources 75 (1998) 130.
[18] J.M. Wang, Y.D. Qian, J.Q. Zhangand, C.N. Cao, J. Appl. Electrochem. 30 (2000) 113.
[19] J.L. Zhu, Y.H. Zhou, C.Q. Gao, J. Power Sources 72 (1998) 231.
[20] Y. Ein-Eli, D. Starosvetsky, M. Auinat, J. Power Sources 114 (2) (2003) 330.
[21] Y. Ein-Eli, M. Auinat, J. Electrochem. Soc. 150 (2003) A1606.
[22] Y. Ein-Eli, M. Auinat, J. Electrochem. Soc. 150 (2003) A1614.
[23] Y. Ein-Eli, Electrochem. Solid State Lett. 7 (2004) B5.
[24] M. Auinat, Y. Ein-Eli, J. Electrochem. Soc. 152 (2005) A1158.
[25] R. Begum, H. Matsuura, J. Chem. Soc., Faraday Trans. 93 (1997) 3839.
[26] S. Lüsse, K. Arnold, Macromolecules 2 (1996) 4251.